First quantitative assessment of the adsorption of a fluorocarbon gas on phospholipid monolayers at the air/water interface

Xianhe Liu, Claire Counil, Da Shi, Estefania Mendoza-Ortega, Andrea Vela-Gonzalez, Armando Maestro, Richard Campbell, Marie Pierre Krafft

First Quantitative Assessment of the Adsorption of a Fluorocarbon Gas on Phospholipid Monolayers at the Air/Water Interface

Xianhe Liu,[a] Claire Counil,[a] Da Shi,[a] Estefania E. Mendoza-Ortega,[a] Andrea V. Vela-Gonzalez,[a] Armando Maestro,[b] Richard A. Campbell,[bc] Marie Pierre Krafft[a]*

[a]University of Strasbourg, Institut Charles Sadron (CNRS), 23 rue du Loess, 67034 Strasbourg Cedex, France

[b]Institut Laue-Langevin, 71 Avenue des Martyrs, CS20156, 38042 Grenoble Cedex 9, France

[c]Division of Pharmacy and Optometry, University of Manchester, Manchester M13 9PT, United Kingdom

*Corresponding author:

Dr. Marie Pierre Krafft

E-mail: krafft@unistra.fr

Tel: +33388414060

Keywords: DPPC; perfluorocarbon; neutron reflectometry; ellipsometry; mixed monolayers; isotopic contrast

ABSTRACT

Hypothesis: Fluorocarbon gases introduced above monolayers of phospholipids at the air/water interface were recently found to promote the adsorption of diverse molecular compounds, with potential application in drug-loaded microbubble design. Quantitative determination of the fluorocarbon present in the monolayers is strongly needed for the development of such applications. We hypothesized that neutron reflectometry (NR) and ellipsometry experiments would allow quantification of the fluorocarbon trapped in the monolayers.

Experiments: We report the first quantitative determination of the extents of adsorption of perfluorohexane (*F*-hexane) on different phospholipid monolayers with respect to both their phase and isotopic form. To this aim, we applied an approach based on co-modeling the data obtained from NR and ellipsometry.

Findings: We found that *F*-hexane adsorbs strongly in monolayers of dipalmitoylphosphatidylcholine (DPPC) when they are both in the liquid expanded (LE) and liquid condensed (LC) phases, but to different extents according to the isotopic form of the phospholipid. Kinetic resolution of the interfacial composition from data on both isotopic contrasts (assuming chemical identicality) was therefore not possible using NR alone, so an alternative NR/ellipsometry co-modeling treatment was applied to data from each isotopic contrast. *F*-hexane adsorbs more abundantly on monolayers of hydrogenous DPPC than chain-deuterated DPPC when they are in the LE phase, whilst the opposite was observed when they monolayers are in the LC phase. The extents of adsorption of *F*-hexane in monolayers of dimyristoylphosphatidylcholine (DMPC, LE phase) and distearoylphosphatidylcholine (DSPC, LC phase) concurs with the strong dependence of those with phospholipids of different isotopic contrasts according to the monolayer phase. This new methodology can lead to advances in the novel characterization of fluorocarbons interacting with phospholipid monolayers of relevance to applications such as in the shells of fluorocarbon-stabilized medically-oriented microbubbles.

1. INTRODUCTION

Several products involving fluorocarbons (*F*Cs), such as microbubbles and vaporizable nanoemulsions, are under clinical evaluation for diverse applications in diagnostic and therapy, including ultrasound imaging modes, non-invasive surgical tissue ablation, sonothrombolysis, potentiation of O_2-dependant cancer treatments such as radio-, chemo- and immunotherapy, blood-brain barrier opening for treatment of central nervous system diseases, etc.[1-7] The *F*C-based colloidal systems most extensively investigated for medical uses comprise *F*C nanoemulsions, nanoemulsions of volatile *F*C that can be converted in microbubbles under various stimuli, and *F*C-stabilized microbubbles. Even so, in spite of the broad interest and applications of *F*C-induced biophysical interactions, quantification of the composition of interfacial layers formed in the presence of *F*Cs, in particular the amount of fluorocarbon that becomes incorporated in the phospholipid monolayer with respect to the phospholipid chain length and hence its phase, has not been achieved to date. Fluorocarbon gases, when introduced in the gas phase above dipalmitoylphosphatidylcholine (DPPC) monolayers, penetrate these monolayers and inhibit their liquid expanded (LE) to liquid condensed (LC) phase transition, that is, the formation of quasi-crystalline LC domains.[8, 9] The *F*C gas can thus restore the re-spreading ability of DPPC molecules at the gas/water interface, enabling their use as active components of lung surfactant replacements.[8] Perfluorohexane (*F*-hexane) has also been shown to induce or accelerate the adsorption at the air/water interface of a range of molecular compounds, including lipids,[10] block co-polymers,[11] proteins,[12] cell biomarkers,[13] cerium oxide,[14] iron oxide nanoparticles,[15] and diamond [16] nanoparticles. This attracting effect of *F*-hexane allowed the recruitment and immobilization of fluorinated cell hypoxia biomarkers[13] and magnetic nanoparticles[15] in the phospholipid shell of microbubbles through fluorine-fluorine hydrophobic forces, without need for covalent binding, thus providing a potential means for delivering the biomarker or nanoparticles through their ultrasound-mediated destruction.

Monolayers of phospholipids, self-supported at the air/water interface, are effective models for investigating the recognition, recruitment, and organization of biological and therapeutic water soluble molecules at interfaces.[17-19] Planar air/water interfaces are also convenient platforms for the application of various techniques, including spectroscopy,[20] rheology,[21] electrochemistry[22] and scattering,[23] and interactions in phospholipid monolayers have been investigated as a function of concentration,[24] pH[25] or temperature.[26] Specular neutron reflectometry (NR) has long been recognized as an effective tool for investigating the structure and composition of mixed layers adsorbed at interfaces.[19, 27-29] This method typically requires co-refined fitting of data acquired with different isotopic contrasts to a common structural model, an approach that usually requires deuterated compounds.

Recent advances in instrumentation have led to the provision of much higher neutron flux than was previously available,[30] in particular at low values of the momentum transfer normal to a reflecting air/water interface (Q_z).[30] This new capability has opened up the quantitative real-time routine monitoring of adsorption kinetics and other dynamic processes in synthetic and biologically-related systems.[31] A recently developed approach involving two parallel neutron reflectivity measurements only at low Q_z values allows one to solve the composition of a binary mixture much faster and more accurately than was formerly possible.[32, 33] An alternative approach to quantify the composition of a binary mixture, but much less exploited, consists of co-modeling data obtained using a single isotopic contrast of NR with data obtained by ellipsometry.[34] To the best of our knowledge, there has been no attempt yet to quantify the adsorption of fluorocarbons on phospholipid monolayers at the air/water interface. Indeed, even though NR is used routinely to investigate interactions of species in the bulk solution with phospholipid monolayers,[35, 36] and has been used to examine the effects on monolayers at the air/water interface from gas phase oxidants,[37, 38] there appears to have been no attempt yet to quantify the adsorption of molecules from the gas phase on monolayers at the air/water interface.

Our goal in this work is to resolve quantitatively the interactions of fluorocarbon gases with planar model phospholipid membranes present in different phases at the air/water interface, which is an essential step to understanding and developing the potential of *F*Cs as reinforcers of microbubble shells for diagnostics and therapy or as components of lung surfactant substitutes. As the low-Q_z method of NR to quantify the interfacial composition of binary mixtures at the air/water interface requires parallel measurements involving components in their native and deuterated forms, and as *F*-hexane has no hydrogen protons, we have performed NR and ellipsometry measurements using hydrogenous DPPC (h-DPPC) and its isotopic analogue bearing d_{62}-perdeuterated acyl chains (d-DPPC), both in the LE and LC phases. NR and ellipsometry data were combined in order to determine the surface excesses of DPPC and *F*-hexane. This study is the first quantitative investigation of the adsorption and incorporation of a fluorocarbon in phospholipid monolayers and also, to our knowledge, the first quantitative assessment of a multi-component system involving adsorption of a component originating from the gas phase.

The manuscript is organized as follows. The principles of NR and ellipsometry are briefly presented in Section II. In Section III, results are presented and discussed: analysis of ellipsometry data recorded in different isotopic contrasts of the same systems reveals that *F*-hexane interacts differently with h- and d-DPPC (III.1); quantitative analysis of NR data of *F*-hexane with h- and d-DPPC monolayers using a standard approach confirms that the assumption of equivalent physical interactions of *F*-hexane with the DPPC isotopic forms is unjustified for this system (III.2); co-modeling NR and ellipsometry data enables quantification of the interfacial composition in both *F*-hexane/h-DPPC and *F*-hexane/d-DPPC mixed monolayers (III.3); in Section IV, adjustment coefficients *R* that were determined for DPPC monolayers in various phases are applied to monolayers of two other phospholipids, dimyristoylphosphatidylcholine (DMPC), which is in the LE phase, and distearoylphosphatidylcholine (DSPC), which is in the LC phase. The results extend our quantification method to different lipid systems while further validating our approach that combines NR and ellipsometry.

II. MATERIALS AND METHODS

1. Materials

1,2-Dimyristoylphosphatidylcholine (h-DMPC), 1,2-dipalmitoylphosphatidylcholine (h-DPPC), 1,2-distearoylphosphatidylcholine (h-DSPC), all >99%, and their chain-deuterated analogues (d_{54}-DMPC; d_{62}-DPPC; and d_{70}-DSPC, all >99%) were purchased from Avanti Polar Lipids (Alabaster, AL, USA) and used without further purification. Perfluorohexane came from Fluorochem (>98%). A Hepes (N-2-(hydroxyethyl)piperazine-N′-(2-ethanesulfonic acid), powder, 99.5%, Corning, NY) buffer (20 mM) in 150 mM NaCl was prepared and adjusted to pH 7.4 using 0.1 N NaOH. Chloroform (99.4%) was purchased from VWR (Avantor, Fontenay-sous-Bois). Ultrapure water was obtained from a Milli-Q (Millipore Corp.) system (surface tension: 72.1 mN m^{-1} at 20°C, resistivity: 18.2 MΩ cm). For the NR experiments, the Hepes buffer was prepared in air contrast matched water (ACMW, containing 8.1% by volume of D_2O (Sigma Aldrich, >99.9% D) in H_2O).

2. Ellipsometry

Ellipsometry is a fast and precise polarized optical reflectometry technique for the characterization of thin films (the film thickness should be smaller than the laser wavelength in the Drude approximation) and the kinetics of adsorption processes.[39, 40] Its footprint is < 1 mm^2, as compared to several cm^2 for NR. Although ellipsometry does not allow direct determination of the surface excesses of multiple components at the interface, it has been used along with NR to perform such quantitative analysis.[34] Ellipsometry measures the change of polarization that light undergoes when it is reflected at an interface. The polarization change is quantified by an amplitude ratio Ψ and a phase shift Δ that are related to the reflection coefficients (parallel r_p and perpendicular r_s to the plane of incidence) by the relation: $r_p/r_s = \tan\Psi\, e^{i\Delta}$. As Ψ is relatively insensitive to thin layers present at the air/water interface, the quantity measured in the present work is the change in phase shift at the interface $\Delta = \Delta_{meas} - \Delta_0$, where Δ_{meas} is the value measured after deposition of the

phospholipid in the presence, or absence, of the fluorocarbon, and Δ_0 the value for the bare air/water interface. This subtraction process approximately eliminates the effects of capillary wave roughness,[41] neglecting the relatively minor influence of the surface tension change from sample to sample. The surface excess Γ can be considered proportional to Δ for layers at the air/water interface in the thin film limit, provided that the thickness increases with Γ with a uniform density (i.e. oil-like behavior).[42] For hydrocarbon surfactants, the relationship between Γ and Δ is approximatively linear.[34] In some cases, however, the linearity is no longer valid, which include LE vs. LC phases of phospholipid monolayers because the technique is sensitive to optical anisotropy[43, 44], layers at the air/water interface in the thin film limit where with increasing surface excess the density increases at uniform thickness,[40] and films thicker than ~10 nm.[39] In the present work, we assume linearity of the $\Gamma(\Delta)$ relationship for fluorocarbon/phospholipid systems in a given phase, as the condensation of the fluorocarbon on a monolayer is expected to result in an increase in thickness rather than density, and we follow the approximation that Δ is an additive function of the amounts of adsorbed compounds.[34] Thus, the phase shift Δ_x of a single component x varies linearly with its surface excess Γ_x; $\Delta_x = k_x \times \Gamma_x$, where k_x is the slope of the linear variation.

In the experiments reported here, Δ measurements were achieved using a phase modulation ellipsometer (Picometer Light Ellipsometer, Beaglehole Instruments, Wellington, NZ) in the Partnership for Soft Condensed Matter (ILL, Grenoble).[45] The ellipsometer was equipped with a HeNe laser with a wavelength of 632 nm and the incidence angle was 50°. The change in phase shift was measured at 5 s time intervals, and then for presentation were averaged over a period of at least 300 s for experiment under air for which stabilization is fast. It took 1.5 h for ellipticity to attain its equilibrium value in the experiments involving the fluorocarbon gas. Data were recorded on h-DPPC and d-DPPC monolayers deposited on the Hepes buffer solutions (11 mL) in Petri dishes (surface area ~30 cm^2) enclosed in a chamber designed at the ILL.[46] The concentrations of the DPPC solutions were the same as those used in the NR measurements, and the dispensed

volumes were adjusted by proportion of the relative surface areas in order to attain identical experimental conditions as in NR. The experiments were repeated at least three times. The experimental errors on Δ measurements were ± 2% for phospholipids exposed to air or *F*-hexane; and ± 3% for experiments involving *F*-hexane alone.

3. **Neutron Reflectometry**

a. Principles of low-Q_z compositional analysis

NR is a powerful tool for the investigation of thin films[47], including phospholipid monolayers, due to the possibility of exploiting isotopic contrast variation.[28, 48-52] The use of ACMW, which has the same neutron scattering length density as air, enables the specular reflectivity signal to arise only from any layer at the interface. The neutron reflectivity profiles show the intensity ratio of neutrons in the specular reflection from the sample to those in the incident beam with respect to the momentum transfer Q_z, as defined by $Q_z = (4\pi \sin \theta)/\lambda$. NR profiles can be modeled to obtain information about the structure and composition of an interfacial layer from the fitted thickness d and scattering length density ρ. However, in our case, the NR data were deliberately acquired only on a restricted Q_z range (0.01–0.03 $Å^{-1}$) and the surface excess of each component at the interface was determined using the low-Q_z compositional analysis method.

In a single component monolayer at the air/water interface, the surface excess is given by $\Gamma_x = \frac{\rho d}{b_x \mathrm{N_A}}$, where b_x is the scattering length of component x and $\mathrm{N_A}$ is Avogadro's constant, ρ is the scattering length density of the component, d is the thickness of the layer. The so-called "scattering excess" of the layer at low Q_z, which is expressed in terms of the amount of interfacial component with respect to its scattering contrast, is thus described as $(\rho d) = \mathrm{N_A} \Gamma_x b_x$. The scattering excess of a mixed layer at low Q_z, expressed in terms of the amount of each interfacial component with respect to its scattering contrast, may be described as $(\rho d) = \mathrm{N_A} \sum \Gamma_x b_x$.[28] This approach is based on the approximation that the scattering contributions of each component is additive as well as the assumption that the interfacial material can be modeled as a single uniform

layer, i.e., low-Q_z nature of the approach is insensitive to any differences in the neutron scattering either in the plane of or normal to the interface. This approximation and assumption are scrutinized below. The reason that this approach was used is that the traditional, structural analysis of NR data over the whole Q_z-range remains too slow currently to resolve the interaction kinetics of interest.

b. Experimental Set-Up

NR measurements were performed using FIGARO (Fluid Interface Grazing Angle ReflectOmeter) reflectometer optimized for horizontal surfaces at the Institut Laue-Langevin (ILL, Grenoble, France).[30] A beam of neutrons with λ = 2−16 Å impinged upon the samples at θ = 0.62°, although a restricted range of λ = 4.5−12 Å was used in the data reduction process to generate reflectivity profiles with a Q_z range of 0.01–0.03 $Å^{-1}$ at a resolution of 8 %. The acquisition time for each sample was 5 min. The data analysis was performed using an arbitrary scattering length density ρ of 5×10^{-6} $Å^{-2}$ with the Motofit program in the Igor software, which allows to obtain the thickness value d.[53] An investigation showed that fitting with refined ρ values instead of the arbitrary value led to small difference (< 3%) in the calculation of the surface excesses of DPPC and *F*-hexane. (see SI "Fitting parameter in low-Q_z analysis", Table S1). It was also verified that our treatment of the data was valid for layer thicknesses lower than 60 Å (see SI, Fig. S1, Table S3, Scheme S3 and Table S8). The layer roughness was set to 3 Å. Six adsorption troughs with sealed lids constructed at the ILL ($11.9 \times 5.0 \times 0.3$ cm^3) were positioned in parallel on a sample changer. ACMW Hepes buffer solutions (18 mL) were deposited in each trough prior to the deposition of a 1-mM solution of the phospholipid (DPPC, DMPC or DSPC) in $CHCl_3$. The gas phase above the monolayers consisted either of air, or of air saturated with *F*-hexane. In the latter case, an open flat aluminum dish ($5.5 \times 8.8 \times 0.5$ cm^3) was filled with 20 mL of liquid *F*-hexane and introduced next to each trough. The measurements were all conducted at 21 ± 1 °C. The saturated vapor pressure and concentration of *F*-hexane at 25°C are 2.9×10^4 Pa (2.3×10^4 Pa at 21°C) and 11.66 mol m^{-3}, respectively; its water solubility is estimated at 2.7×10^{-4} mol m^{-3} at 25°C.[54-56]

The saturation of the atmosphere in the trough was confirmed for each experiment by the presence of some liquid *F*-hexane still left in the dish when the lids were removed.

Because the surface pressure π could not be measured in the adsorption troughs during NR measurements, we determined in advance of the neutron experiment the variation of π as a function of the DPPC spread volume, under air or *F*-hexane exposure in a trough similar to those used on FIGARO and at the same temperature (21 ± 1°C, SI, Fig. S2a). This procedure allowed reconstruction of the π/A isotherms for DPPC monolayers investigated during the NR experiments (SI, Fig. S2b). Various volumes of DPPC solution were deposited in order to provide monolayers in the LE phase (8 and 10 µL), in the LE-LC coexistence phase (12 and 14 µL) and in the LC phase (16 µL) (SI, Table S4). It was verified that h- and d-DPPC monolayers were in comparable physical state under air and under *F*-hexane exposure for the same deposited volume, hence same molecular area (SI, Fig. S3a). Appropriate spread volumes of DMPC solutions in $CHCl_3$ (15 µL) or DSPC (26 µL) provided monolayers at 35 mN m^{-1}, which corresponds to the LE phase for DMPC and to the LC phase for DSPC (SI, Fig. S3b,c). The lids of the troughs were closed and the NR measurements were conducted for 6 h. For the experiments in which *F*-hexane was present, the lids were opened after the 6 h-period of monitoring in order to vent *F*-hexane out of the system. The measurements were then resumed for another 2 h period. Neutron reflectivity profiles of the adsorption of *F*-hexane at the surface of the Hepes buffer were also measured in the absence of phospholipid. The experiments were repeated at least three times. Experimental errors on the surface excesses of DPPC (Γ_{DPPC}) are estimated ≤ 7% (± 0.1 µmol m^{-2} for LE phase and ± 0.2 µmol m^{-2} for LC phase), and ~6% (± 1.0 µmol m^{-2}) for *F*-hexane ($\Gamma_{F-\mathrm{hex}}$).

III. RESULTS AND DISCUSSION

1. **Ellipsometry Reveals a Difference in *F*-hexane Interactions with h-DPPC and d-DPPC**

Ellipsometry was initially used in order to examine two isotopic forms of DPPC monolayer both in air and when exposed to *F*-hexane saturated air. The variation of the phase shift Δ_{meas} was monitored

over time for monolayers of h- and d-DPPC in the LE and LC phases and under air or *F*-hexane-saturated air (Fig. 1ab). The adsorption of *F*-hexane on the surface of the aqueous phase (*i.e.* in the absence of phospholipid) was also monitored (Fig. 1c). In air (Fig. 1a), we observe that 1) Δ_{meas} is higher for DPPC monolayers in the LC than in the LE phase, which is expected because the surface excess Γ is higher (spread values correspond to $\Gamma =$ 2.8 vs. 1.7 µmol m^{-2} for the LC and LE phases, respectively); 2) Δ_{meas} does not exhibit a rising or falling trend over time; and 3) Δ_{meas} depends only slightly on the DPPC isotopic form (2.26 ± 0.05° and 2.19 ± 0.05° for h- and d-DPPC in the LE phase; and 3.03 ± 0.05° and 2.82 ± 0.05° in the LC phase). By contrast, when the DPPC monolayers are exposed to *F*-hexane (Fig. 1b), two significant differences are observed. First, Δ_{meas} is no longer constant over time as its adsorption is progressive. This can result from the fact that the adsorption of *F*-hexane decreases the value of Δ because *F*-hexane has a smaller refractive index than water (1.251 [57] vs. 1.333; Fig. 1c). Second, Δ_{meas} is no longer the same for the two isotopic forms. In both LE and LC states, Δ_{meas} is lower for d-DPPC than for h-DPPC throughout the adsorption time period (Fig. 1b). In the LE phase, the Δ_{meas} minimum values were 1.32° and 1.87° for d-DPPC and h-DPPC, respectively (*i.e.* a difference of 0.55°), indicating higher adsorption of *F*-hexane on d-DPPC monolayer. In the LC phase, the difference was lower (0.27°; with Δ minimum values of 2.29° and 2.02° for d-DPPC and h-DPPC, respectively).

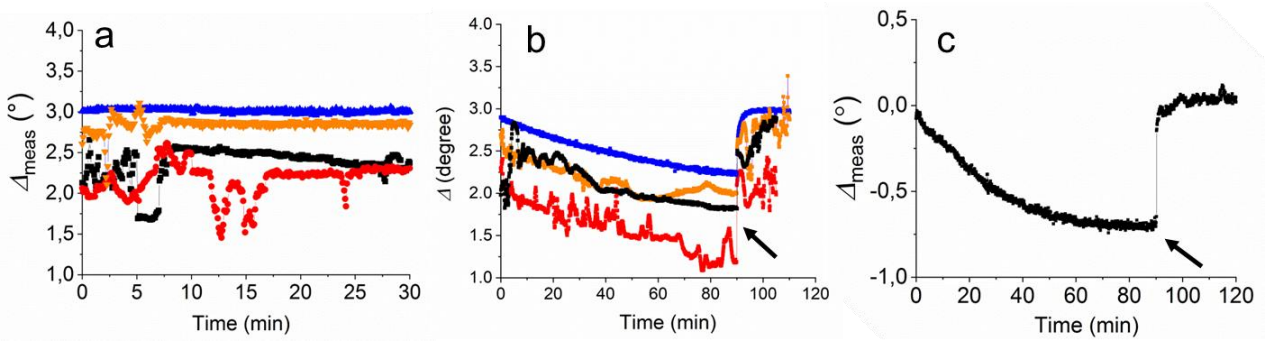

Figure 1. Variation of the phase shift Δ_{meas} over time, as measured by ellipsometry for DPPC monolayers in the LE phase (black: h-DPPC; red: d-DPPC) and LC phase (blue: h-DPPC; orange:

d-DPPC) under a) air and b) *F*-hexane exposure. c) Variation of Δ_{meas} over time for *F*-hexane adsorption on the aqueous phase in the absence of phospholipid. The arrows indicate the time point at which *F*-hexane was vented-off. The experimental errors were ± 2% for DPPC monolayers exposed to air or to *F*-hexane; and ± 3% for *F*-hexane adsorbing at the surface of the aqueous phase.

It is known that the difference between the refractive indices of h- and d-hydrocarbons decreases when their carbon atom number increases,[58] thus resulting in a strong decrease of the proportional change in $\Delta n = n - n_{water}$ (n and n_{water} being the refractive indices of a given hydrocarbon and water, respectively) for h-and d-hydrocarbons. It is likely that for long hydrocarbon chains such as those of DPPC, this proportional change becomes negligible. As a consequence, any difference in the ellipsometry data can be attributed to different extents of interaction of *F*-hexane to h- and d-DPPC. These results show that isotopic effects are observed for DPPC monolayers in LE and LC states, with *F*-hexane interacting more strongly with d-DPPC than with h-DPPC. It is noted that when *F*-hexane is vented-off from the adsorption trough, Δ_{meas} returns back to its initial value, that is, to that measured in the absence of the fluorocarbon, which demonstrates that the DPPC/*F*-hexane interactions are reversible. Quantification of these effects was needed, as described in Section 3.

2. Quantitative Analysis by Neutron Reflectometry Confirms the Difference in *F*-hexane Interactions with h-DPPC and d-DPPC

To confirm and explore the implication of the isotope effects suggested by the ellipsometry data presented above, neutron reflectivity profiles of h-DPPC and d-DPPC monolayers were measured in air and under *F*-hexane exposure in the low-Q_z range (0.01-0.03 Å^{-1}) (Fig. 2).

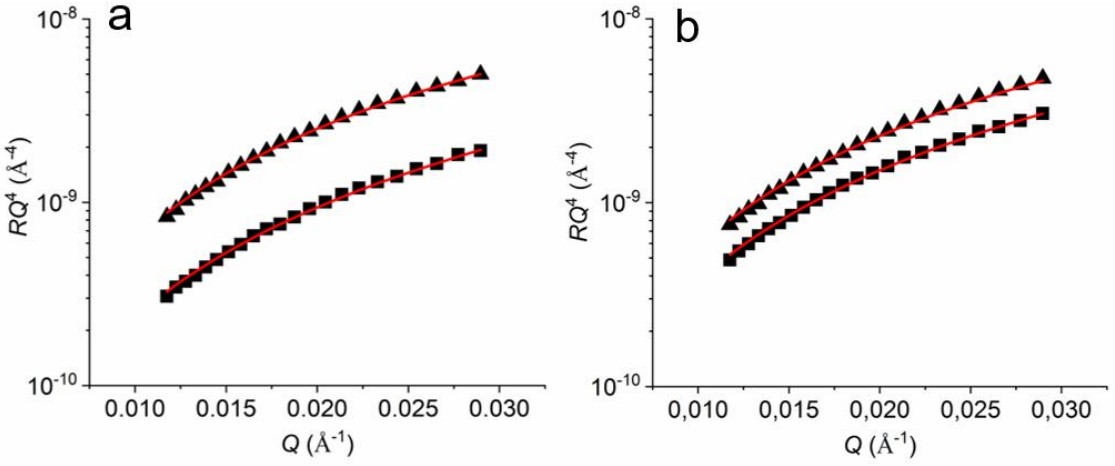

Figure 2. Measured (h-DPPC: squares; d-DPPC: triangles) and fitted (red line) variation of RQ^4 as a function of Q_z of DPPC monolayers exposed to *F*-hexane a) in the LE phase and b) in the LC phase at the adsorption equilibrium (at ~4 h).

First, for reference, the data were modeled using a standard treatment, that is, assuming that *F*-hexane interacts *to the same extent* with h- and d-DPPC monolayers, and that the resulting layers are *homogeneous*. The surface excesses of h-DPPC ($\Gamma_{\text{h-DPPC}}$) and d-DPPC ($\Gamma_{\text{d-DPPC}}$) and the surface excesses of *F*-hexane when interacting with h-DPPC and d-DPPC, ($\Gamma_{F\text{-hex/h-DPPC}}$ and $\Gamma_{F\text{-hex/d-DPPC}}$) are given in the following equations**:**

$$(\rho d)_{\text{h-DPPC}}^{F-\text{hex.}} = N_{\text{A}} \left(\Gamma_{\text{h-DPPC}} \times b_{\text{h-DPPC}} + \Gamma_{F\text{-hex/h-DPPC}} \times b_{F\text{-hex}}\right) \qquad \text{Eq. 1}$$

$$(\rho d)_{\text{d-DPPC}}^{F-\text{hex.}} = N_{\text{A}} \left(\Gamma_{\text{d-DPPC}} \times b_{\text{d-DPPC}} + \Gamma_{F\text{-hex/d-DPPC}} \times b_{F\text{-hex}}\right) \qquad \text{Eq. 2}$$

where $(\rho d)_{\text{h-DPPC}}^{F-\text{hex.}}$ and $(\rho d)_{\text{d-DPPC}}^{F-\text{hex.}}$ are the scattering excesses of the h- and d-DPPC monolayers exposed to *F*-hexane; $b_{\text{h-DPPC}}$, $b_{\text{d-DPPC}}$ and $b_{F\text{-hex}}$ are the scattering lengths of h-DPPC (27.55 fm), d-DPPC (673.03 fm) and *F*-hexane (117.772 fm), respectively. Under air, Γ_{DPPC} is calculated with equations 1 and 2 with $\Gamma_{F\text{-hex/h-DPPC}} = \Gamma_{F\text{-hex/d-DPPC}} = 0$. As $\Gamma_{\text{h-DPPC}}$ and $\Gamma_{\text{d-DPPC}}$ are assumed to be equal (same quantities of h-DPPC and d-DPPC were deposited; noted Γ_{DPPC} below) and as $\Gamma_{F\text{-hex/h-DPPC}}$ and $\Gamma_{F\text{-hex/d-DPPC}}$ are also equal (our hypothesis), Eqs. 1 & 2 can be resolved to calculate Γ_{DPPC} and $\Gamma_{\text{F-hex}}$.

It is observed that for monolayers in the LE phase under *F*-hexane exposure (Fig. 3a), based on the above assumptions, Γ_{DPPC} would be higher than the value measured under air (2.1 vs. 1.7 µmol m^{-2}, ± 0.2 µmol m^{-2}), and also higher than the value that corresponds to the amount of phospholipid deposited (1.7 µmol m^{-2}), which is physically unrealistic. In the LC phase (Fig. 3b), Γ_{DPPC} was found to be lower than the value under air and the deposited value, a result that could be explained by a desorption of DPPC by *F*-hexane, which would be caused either by 3D collapse or solubilization of phospholipid molecules in the sub-phase in the form of vesicles. The latter hypothesis is unlikely as

3D collapse of bilayers on top of a DPPC monolayer has never been observed in previous investigations by fluorescence microscopy or SAXS.[59, 60] On the contrary, all these previous investigations demonstrated that the *F*C gas causes a fluidization of the DPPC monolayer, even at high surface pressure, and dissolution of DPPC liquid condensed phase domains.[59, 60]

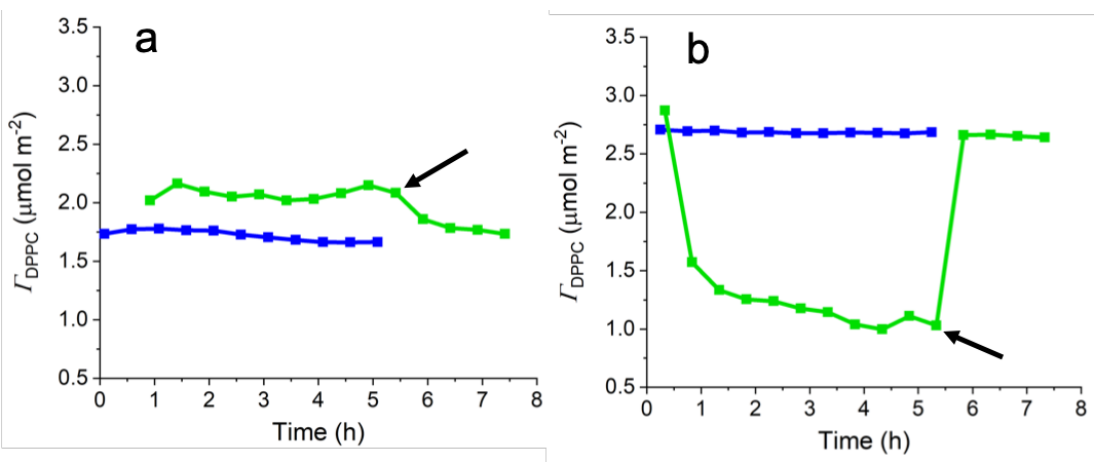

Figure 3. Variation of DPPC surface excess, Γ_{DPPC}, over time for DPPC monolayers in a) the LE phase and b) the LC phase, under air (blue) and under *F*-hexane exposure (green). Γ_{DPPC} is calculated with the assumption that the interactions between *F*-hexane and DPPC isotopic forms are identical. The arrows indicate when *F*-hexane has been vented off from the system. Errors on Γ_{DPPC} were ± 0.2 µmol m^{-2}.

Whilst it would be intuitive on the basis of the ellipsometry results above to attribute these physically unrealistic results to limitations of the analysis method applied in that *F*-hexane is interacting with h-DPPC and d-DPPC to different extents, we went on to scrutinize whether our assumption of modeling the low-Q_z data as a single, uniform layer could instead explain, or at least contribute, to the unphysical nature of the results above. The possible effects of non-uniformity in the direction normal to the interface (i.e. different locations of *F*-hexane either in a layer above or mixed in with the lipid chains, themselves in a layer above solvated headgroups), or non-uniformity in the direction lateral to the interface (i.e. the possibility of domains of *F*-hexane sitting in between regions of lipid monolayer on a length scale above the coherence length of the neutrons) were examined. These tests scrutinized the insensitivity to the interfacial structure of the low-Q_z analysis method and indeed went beyond lengths taken to validate the approach in any such previous study. The tests were performed by simulating neutron reflectivity data of the mixed *F*-hexane/lipid systems in different

isotopic contrasts using a structural model and parameters that had been validated using data recorded in 4 isotopic contrasts over the fully accessible Q_z-range,[33] before applying the low-Q_z analysis method to the same restricted Q_z-range using the same approach as described herein. More information can be found in the Supporting Information (SI p. S5 "Simulation of the Effect of Vertical Separation" and p. S9 "Simulation of the Effect of Lateral Separation").

The results of the simulations revealed that a vertical separation of the scattering length density profile resulting from stratification of the *F*-hexane (of different locations), lipid chains and solvated lipid headgroups normal to the interface results in a maximum uncertainty in the resulting interfacial composition of 3% for DPPC and 6% for *F*-hexane, and that use of a heterogeneous model to mimic lateral separation made the unphysical nature of the resulting DPPC surface excess even more pronounced. These simulations also serve to validate the use of the low-Q_z analysis method with a single, uniform layer model in our case, as there is no indication that a laterally-heterogeneous model is more appropriate, uncertainties introduced from the additivity approximation about the scattering from different components are minimal, and fits to the experimental data were significantly poorer when the lateral domain thickness of *F*-hexane was consistent with full lateral separation of the interfacial components.

We thus conclude that the physically unrealistic data above are not the result of vertical or lateral heterogeneity that would invalidate use of a single uniform layer in the low-Q_z data analysis, but instead that *F*-hexane indeed interacts to different extents with the two isotopic forms of DPPC, as indicated by ellipsometry in Section 1. It is interesting to note that phospholipid monolayers do not generally exhibit strong isotopic effects, as lipophilic attraction between hydrocarbon chains is the main driving force of monolayer dynamics.[61] However, the interaction energies associated with H-bonds and D-bonds are different, which has pronounced effect on the phase transitions in phospholipid mono- and bilayers,[48, 62-65] and may help to explain the present results.

3. Co-modeling Ellipsometry and NR Data

In Section 2, we have observed that, owing to the difference in interactions of *F*-hexane with the two isotopic forms of DPPC, the low-Q_z analysis method of NR alone – i.e. solving the surface excess of two components by making measurements in two different isotopic contrasts using Eqs 1 and 2 – is not sufficient to resolve the interfacial composition of the system because the assumption that the interfacial composition is the same in the two measurements is not valid. An alternative approach to resolve quantitatively the composition of a binary mixture is to co-model data from one NR measurement in a single isotopic contrast and one ellipsometry measurement, as described by Bain *et al*.[34]

We have applied this approach for NR and ellipsometry data recorded for h- and d-DPPC under air and *F*-hexane-saturated air in order to treat the systems of different isotopic contrasts individually. The phase shifts of h- and d-DPPC monolayers under *F*-hexane exposure, as measured by ellipsometry, are given by Eq. 3 & 4:

$$\Delta_{h-DPPC}^{F-hex} = k_{\mathrm{h-DPPC}} \times \Gamma_{\mathrm{h-DPPC}} + k_{F-\mathrm{hex}} \times \Gamma_{F-\mathrm{hex/h-DPPC}} \quad \text{Eq. 3}$$

$$\Delta_{d-DPPC}^{F-hex} = k_{\mathrm{d-DPPC}} \times \Gamma_{\mathrm{d-DPPC}} + k_{F-\mathrm{hex}} \times \Gamma_{F-\mathrm{hex/d-DPPC}} \quad \text{Eq. 4}$$

where Δ_{h-DPPC}^{F-hex} and Δ_{d-DPPC}^{F-hex} are the phase shifts of h- and d-DPPC monolayers under *F*-hexane as measured by ellipsometry (average of values over 1 h taken after equilibrium reached after 1.5 h). $k_{\mathrm{h-DPPC}}$, $k_{\mathrm{d-DPPC}}$ and $k_{F-\mathrm{hex}}$ are the slopes of the linear variations of Δ as a function of Γ, were obtained in the single-components systems using the equation $k_x = \Delta_x/\Gamma_x$, where Δ_x was measured by ellipsometry and Γ_x by NR.

Results, collected in Table 1, show that the *k* values are influenced mainly by the phase of the monolayer, LE versus LC, as reported earlier and ascribed to monolayer optical anisotropy.[43, 44, 66] On the other hand, the values are not much influenced by the isotopic form.

Table 1. Phase shift Δ (from ellipsometry) and surface excess Γ (from NR) of hydrogenous and deuterated DPPC monolayers under air, and of an adsorbed layer of *F*-hexane in the absence of phospholipids; *k* values are the slope of the linear variation of Δ as a function of Γ.

	Phase shift Δ (°)	Surface excess Γ (µmol m^{-2})	k
h-DPPC (LE)	2.26 ± 0.05	1.6 ± 0.1	1.4
d-DPPC (LE)	2.19 ± 0.05		1.4
h-DPPC (LC)	3.03 ± 0.05	2.8 ± 0.2	1.1
d-DPPC (LC)	2.82 ± 0.05		1.0
F-hexane	-0.7 ± 0.02	19.0 ± 1.0	-0.04

These k values were used for the calculation of surface excesses in DPPC/*F*-hexane monolayers. Co-modeling NR and ellipsometry data for *F*-hexane adsorption on h- and d-DPPC monolayers in LE and LC phases, led to the values of $\Gamma_{\text{h-DPPC}}$, $\Gamma_{\text{d-DPPC}}$, $\Gamma_{F\text{-hex/h-DPPC}}$, and $\Gamma_{F\text{-hex/d-DPPC}}$ (using Eqs. 1 & 3 for h- DPPC and Eqs. 2 & 4 for d-DPPC). It is seen in Figure 4a that, for each physical state, $\Gamma_{\text{h-DPPC}}$ and $\Gamma_{\text{d-DPPC}}$ are approximately identical (difference within the experimental error), and constant over time, whether the DPPC monolayers are exposed to air or to *F*-hexane. This shows that the co-modeling method, independent of the isotopic effect, permits accurate calculation of DPPC surface excesses. The surface excesses correspond well to the quantities deposited, which endorses the fact that the extent of the interactions of *F*-hexane depends on the isotopic form. It is also observed that *F*-hexane always adsorbs strongly on DPPC monolayers. The surface excess of the fluorocarbon is higher on d-DPPC than on h-DPPC monolayers in the LE phase (20.0 vs. 16.8 µmol m^{-2}, respectively; ± 1.0 µmol m^{-2}), while it is lower in the LC phase (13.5 vs. 20.8 µmol m^{-2}, respectively, ± 1.0 µmol m^{-2}) (Fig. 4b). This confirms that the interactions of the fluorocarbon are different with the hydrogenous or deuterated phospholipid, and suggests that the extents of interaction are also influenced by the phase of the DPPC monolayers. The adjustment coefficient $\Gamma_{F\text{-hex/h-DPPC}}/\Gamma_{F\text{-hex/d-DPPC}}$ ratio, R, is ~0.84 in the LE phase, and ~1.73 in the LC phase.

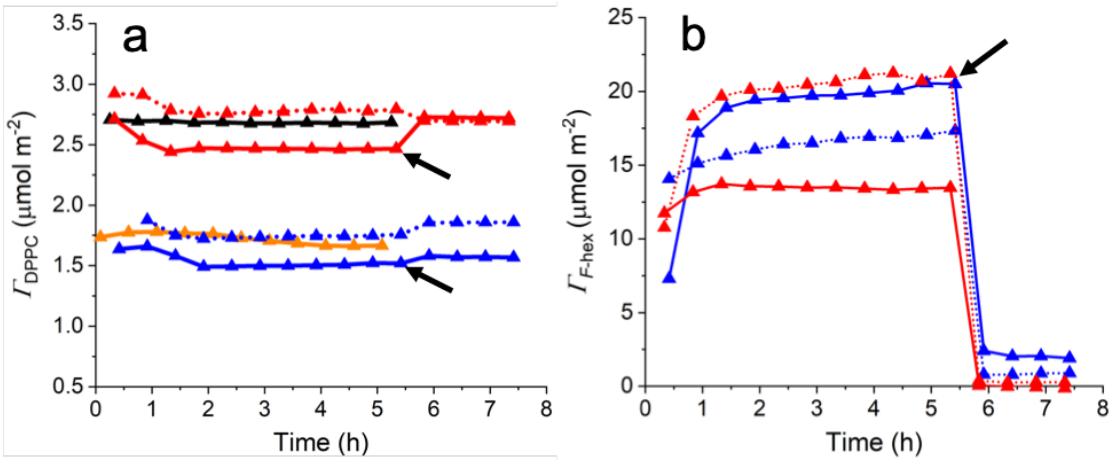

Figure 4. a) Variation of DPPC surface excesses, $\Gamma_{\mathrm{h-DPPC}}$ (dotted lines) and $\Gamma_{\mathrm{d-DPPC}}$ (solid lines) over time for monolayers in the LE phase in air (orange) and under *F*-hexane (blue), and in the LC phase in air (black) and under *F*-hexane (red). b) Variation of $\Gamma_{F-\mathrm{hex}}$ adsorbed over time on h-DPPC (dotted line) and d-DPPC monolayers (solid line) in the LE (blue) and LC (red) phases. The arrow indicates when *F*-hexane has been vented off from the system. Errors on Γ_{DPPC} and $\Gamma_{F-\mathrm{hex}}$ were ± 0.2 and ± 1.0 µmol m^{-2}, respectively.

Based on the result that the surface excesses of DPPC under *F*-hexane and under air are close, as calculated by co-modeling ellipsometry and NR data, the values of $\Gamma_{F\text{-hex/h-DPPC}}$ and $\Gamma_{F\text{-hex/d-DPPC}}$, and hence the values of *R* for various surface pressures were calculated using the NR data, by fixing Γ_{DPPC} to its value in air. The results, collected in Figure 5, show the variation of *R* as a function of molecular area.

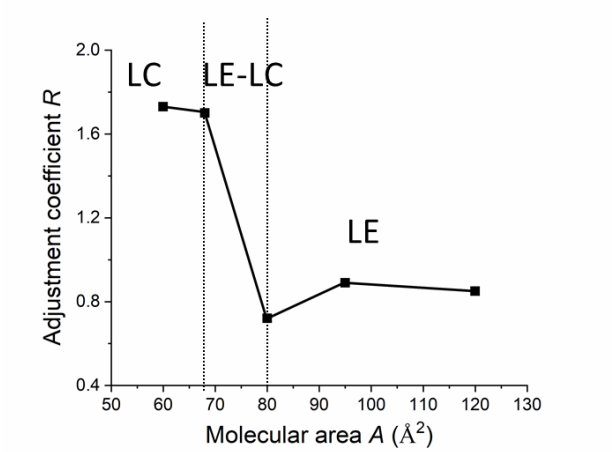

Figure 5. Variation of the adjustment coefficient *R* for DPPC monolayers under *F*-hexane as a function of molecular area *A*.

We observe a clear trend that *R* is dependent on the physical state of DPPC layers: in the LE phase, $R < 1$, reflecting the weaker interactions developed between *F*-hexane with h-DPPC than with d-DPPC; whereas in the LC phase, $R > 1$, reflecting that the interactions of *F*-hexane with h-DPPC are stronger. Different strengths of *F*-hexane interactions with hydrogenous and deuterated lipids in both the LE and LC phases were thus evidenced. Deuteration results in a decrease of the intermolecular interactions among phospholipids, which is the reason why gel-to-fluid transition phase temperatures are depressed in bilayers.[67] As a consequence, *F*-hexane can more easily

accommodate in d-DPPC monolayers than in h-DPPC ones in disorganized LE phase and in the coexistence region. The reverse tendency observed in the organized LC phase may be related to the fact that the interactions between C-F and C-H or C-D bonds can differ. For example, it has been found that plasticization of a semi-crystalline polymer (poly(vinyl alcohol) by glycerol in the presence of a surfactant was dependent on the isotopic form of the plasticizer.[68]

4. Extension to Other Phospholipids

In order to investigate the breath and robustness of the methodology and extend the results obtained with DPPC to other systems, we investigated the interactions of *F*-hexane with two other phospholipids, dimyristoylphosphatidylcholine (DMPC) and distearoylphosphatidylcholine (DSPC). By contrast with DPPC, DMPC and DSPC monolayers do not experience phase transitions at room temperature, and are in the LE and LC states, respectively, at the chosen surface pressure (35 mN m^{-1}; Fig. S2b,c). As for DPPC, the assumption that the fluorocarbon gas interacts similarly with the two isotopic forms led to phospholipid surface excesses that were higher than the values measured under air for the DMPC monolayers (LE phase), and lower for the DSPC monolayers (LC phase) (Fig. 6ab), which is physically unrealistic in the case of DMPC, and would mean, in the case of DSPC, that the phospholipid desorbs from the surface, which is unlikely for the reasons discussed above.

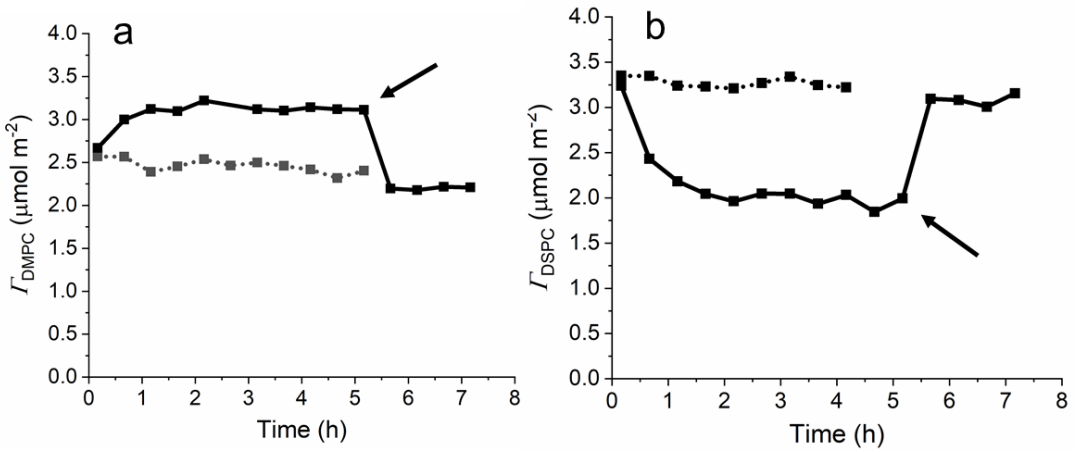

Figure 6. Variation of surface excesses Γ_{DMPC} and Γ_{DSPC} as a function of time for a) a DMPC monolayer (LE phase, 35 mN m^{-1}) and b) a DSPC monolayer (LC phase, 30 mN m^{-1}) under air (dotted line) and under *F*-hexane exposure (solid line). In both cases, the surface excesses are calculated with the assumption of identical interactions between *F*-hexane and the two isotopic phospholipid forms.

The arrows indicate when *F*-hexane has been vented off from the system. Errors on Γ_{DPPC} were ± 0.2 µmol m^{-2}.

We have therefore used the ratio *R* determined in the DPPC LE phase and LC phase, respectively, that was found to be sensitive to the physical state of the monolayers to determine the adjusted surface excesses of DMPC and DSPC according to:

$$(\rho d)_{\mathrm{h-PL}}^{F-\mathrm{hex.}} = N_{\mathrm{A}} \left(\Gamma_{\mathrm{PL}} \times b_{\mathrm{h\text{-}PL}} + R \times \Gamma_{F\text{-hex/d-PL}} \times b_{F\text{-hex}}\right) \qquad \textbf{Eq. 5}$$

$$(\rho d)_{\mathrm{d-PL}}^{F-\mathrm{hex.}} = N_{\mathrm{A}} \left(\Gamma_{\mathrm{PL}} \times b_{\mathrm{d\text{-}PL}} + \Gamma_{F\text{-hex/d-PL}} \times b_{F\text{-hex}}\right) \qquad \textbf{Eq. 6}$$

where $(\rho d)_{\mathrm{h-PL}}^{F-\mathrm{hex.}}$ and $(\rho d)_{\mathrm{d-PL}}^{F-\mathrm{hex.}}$ are the scattering excesses of h- and d-phospholipid monolayers (DMPC or DSPC) exposed to *F*-hexane. Γ_{PL} is the surface excess of phospholipid. $\Gamma_{F\text{-hex/d-PL}}$ and $\Gamma_{F\text{-hex/d-PL}}$ are the surface excesses of *F*-hexane interacting with h- or d-phospholipid.

The results show that, once adjusted, the phospholipid surface excesses are again close to the deposited values and to the values measured under air within the experimental error (± 0.2 µmol m^{-2}) for both DMPC and DSPC (Fig. 7ab). Enhanced interactions of *F*-hexane with d-phospholipid were observed for DMPC in the LE phase, while interactions with the h-phospholipid were higher for DSPC in the LC phase. These results further validate our approach based on co-modeling data of NR and ellipsometry. They also indicate that the isotopic effect of the interaction of *F*-hexane and phospholipids, is strongly influenced by the phase of the monolayers, which is quantified directly herein for the first time.

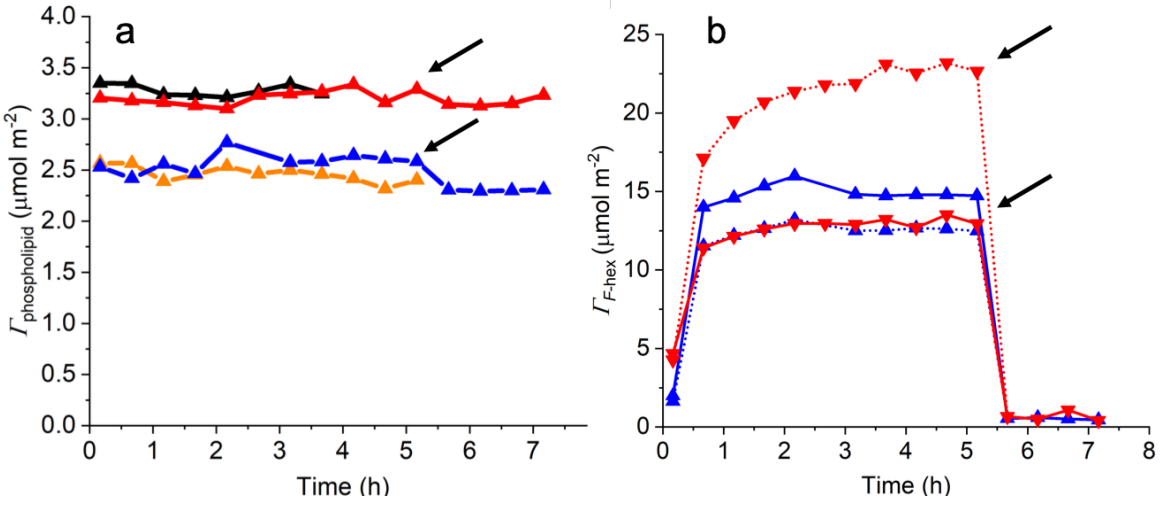

Figure 7. a) Variation of Γ_{DMPC} over time for DMPC monolayers (LE phase) under air (orange) or under *F*-hexane (blue), and of Γ_{DSPC} for DSPC monolayers (LC phase) under air (black) or under *F*-hexane (red). b) Variation of $\Gamma_{F-\mathrm{hex}}$ adsorbed over time on h-DMPC (blue, dotted line) and d-DMPC monolayers (blue, solid line) in the LE phase; and on h-DSPC (red, dotted line) and d-DSPC monolayers (red, solid line) in the LC phase. The arrow indicates when *F*-hexane was vented off from the system. Errors on Γ_{DPPC} and $\Gamma_{F-\mathrm{hex}}$ were ± 0.2 and ± 1.0 µmol m^{-2}, respectively.

IV. CONCLUSIONS AND PERSPECTIVES

We have combined neutron reflectometry/ellipsometry data to quantify, for the first time, the extents of interaction of a fluorocarbon gas with different phospholipid monolayers with respect to their phase and isotopic contrast. This is also the first time the interfacial composition of a mixed system in which vapor adsorbs to a monolayer at the air/water interface has been resolved directly to our knowledge. The systems under investigation were DMPC, DPPC and DSPC monolayers exposed to a saturated atmosphere of *F*-hexane, and the interactions were resolved in real time.

The *a priori* hypothesis that the interactions of *F*-hexane with two isotopic forms of the phospholipids are the same was shown not to be valid. Differences in the extent of phospholipid monolayer/fluorocarbon gas interactions with respect to the isotopic contrast therefore could not be resolved in real time using an establish approach of neutron reflectometry alone, and instead was quantified by co-modeling neutron reflectometry and ellipsometry data. We were thus able to calculate phospholipid surface excesses during the *F*-hexane interactions that not only matched the deposited amounts but also matched the values determined under air. We also scrutinized the physical basis of the low-Q_z analysis method of neutron reflectometry to demonstrate its suitability for purpose in the present work to a greater depth than in any other study since its development a few years ago.[28, 32] The co-modeling methodology also allowed us to quantify the strong *F*-hexane adsorption on different phospholipid monolayers. The extents of interaction depend primarily on the isotopic form of the phospholipid and on the phase of the monolayers. Monolayers of DMPC and DPPC in the liquid expanded phase experience the highest fluorocarbon adsorption when they are in deuterated form, which can be explained by the fact that the monolayers of deuterated phospholipids

are less cohesive. On the other hand, monolayers of DPPC and DSPC in the liquid condensed phase experience the highest fluorocarbon adsorption when they are in their native hydrogenous form, a difference in behavior that may be related to the difference in energies of interactions between C-F and C-H and C-D bonds. This inference is in keeping with pronounced isotopic effects on the phase transitions in phospholipid mono- and bilayers [48, 62-65], and is a matter that warrants further investigation.

More generally, these results open up quantification of the attraction to monolayers exerted by supernatant fluorocarbon gases vis-à-vis molecular compounds such as drugs, surfactants, copolymers, and others, present in the aqueous sub-phase, which has not been studied to date. We envisage that this quantification will be applicable in the case of medical microbubbles, which have a shell of phospholipids and are stabilized by fluorocarbons. The nature of the fluorocarbon, and hence its concentration in the bubble shell, may be key to control microbubble size and stability characteristics, as well as the ability of the microbubble shell to accommodate actives and drugs. The new methodology established in the present work can therefore lead to the development and optimization of emerging medical applications that has not been possible to contemplate until now.

Acknowledgements: The authors are grateful to various institutions for their financial support: the French National Agency for Research (ANR, PatMol Project, Ph. D fellowship for X.L.), the Strasbourg Foundation for Research in Chemistry (icFRC, Ph. D fellowship for C.C.); the INTERREG V program (Nanotransmed Project; Ph. D fellowship for D.S.); the CONACYT (Mexico, Ph. D fellowships for E.E.M.-O. (grant #459199) and A.A.V.-G. (grant # 459202). X.L., E.E.M.-O. are grateful to the GIS Fluor for travel grants. We also thank the Institut Laue-Langevin for beam time on FIGARO (DOI: https://doi.ill.fr/10.5291/ILL-DATA.9-13-772), as well as the Partnership for Soft Condensed Matter for use of the ellipsometer.

V. REFERENCES

[1] E.S. Schutt, D.H. Klein, R.M. Mattrey, J.G. Riess, Injectable microbubbles as contrast agents for diagnostic ultrasound imaging: The key role of perfluorochemicals, Angew. Chem. Int. Ed. 42 (2003) 3218-3235.

[2] J.R. Lindner, Microbubbles in medical imaging: Current applications and future directions., Nat. Rev. Drug Disc. 3 (2004) 527-532.

[3] L. Abou-Elkacem, S.V. Bachawal, J.K. Willmann, Ultrasound molecular imaging: Moving toward clinical translation, Eur. J. Radiol. 84 (2015) 1685–1693.

[4] S. Wang, J. Hossack, A.L. Klibanov, Targeting of microbubbles: contrast agents for ultrasound molecular imaging., J. Drug Target. 26 (2018) 420-434.

[5] K. Graham, E. Unger, Overcoming tumor hypoxia as a barrier to radiotherapy, chemotherapy and immunotherapy in cancer treatment, Intl. J. Nanomed. 13 (2018) 6049–6058.

[6] A. Sahu, I. Kwon, G. Tae, Improving cancer therapy through the nanomaterials-assisted alleviation of hypoxia, Biomaterials 228 (2020) 119578.

[7] M.P. Krafft, Alleviating tumor hypoxia with perfluorocarbon-based oxygen carriers, Curr. Opin. Pharmacol. 53 (2020) 117-125.

[8] M.P. Krafft, Overcoming inactivation of the lung surfactant by serum proteins: a potential role for fluorocarbons?, Soft Matter 11 (2015) 5982-5994.

[9] D. Shi, X. Liu, C. Counil, M.P. Krafft, Fluorocarbon exposure mode markedly affects phospholipid monolayer behavior at the gas/liquid interface: Impact on size and stability of microbubbles, Langmuir 35 (2019) 10025-10033.

[10] P.N. Nguyen, T.T. Trinh Dang, G. Waton, T. Vandamme, M.P. Krafft, A nonpolar, nonamphiphilic molecule can accelerate adsorption of phospholipids and lower their surface tension at the air/water interface ChemPhysChem 12 (2011) 2646-2652.

[11] Y. Ando, H. Tabata, M. Sanchez, A. Cagna, D. Koyama, M.P. Krafft, Microbubbles with a self-assembled poloxamer shell and a fluorocarbon inner gas, Langmuir 32 (2016) 12461-12467.

[12] L. Gazzera, R. Milani, L. Pirrie, M. Schmutz, C. Blanck, G. Resnati, P. Metrangolo, M.P. Krafft, Design of highly stable echogenic microbubbles through controlled assembly of their hydrophobin shell, Angew. Chem. Int. Ed. 55 (2016) 10263-10267.

[13] G. Yang, M. O'Duill, V. Gouverneur, M.P. Krafft, Recruitment and immobilization of a fluorinated biomarker across an interfacial phospholipid film using a fluorocarbon gas, Angew. Chem. Int. Ed. 54 (2015) 8402-8406.

[14] C. Justeau, A.V. Vela-Gonzalez, A. Jourdan, J.G. Riess, M.P. Krafft, Adsorption of cerium salts and cerium oxide nanoparticles on microbubbles can be induced by a fluorocarbon gas, ACS Sustain. Chem. Eng. 6 (2018) 11450-11456.

[15] D. Shi, J. Wallyn, D.-V. Nguyen, F. Perton, D. Felder-Flesch, S. Bégin-Colin, M. Maaloum, M.P. Krafft, Microbubbles decorated with dendronized magnetic nanoparticles for biomedical imaging. Effective stabilization via fluorous interactions, Beilstein J. Nanotechnol. 10 (2019) 2103-2115.

[16] E.E. Mendoza-Ortega, M. Dubois, M.P. Krafft, Fluorocarbon gas exposure induces disaggregation of nanodiamond clusters and enhanced adsorption, enabling medical microbubble formation, ACS Appl. Nano Mater. 3 (2020) 8897-8905.

[17] K. Ariga, T. Kunitake, Molecular recognition at air-water and related interfaces: complementary hydrogen bonding and multisite interaction, Acc. Chem. Res. 31 (1998) 371-378.

[18] K. Ariga, T. Nakanishi, J.P. Hill, A paradigm shift in the field of molecular recognition at the air–water interface: from static to dynamic, Soft Matter 2 (2006) 465-477.

[19] L.A. Clifton, R.A. Campbell, F. Sebastiani, J. Campos-Terán, J.F. Gonzalez-Martinez, S. Björklund, J. Sotres, M. Cárdenas, Design and use of model membranes to study biomolecular interactions using complementary surface-sensitive techniques, Adv. Colloid Interface Sci. 277 (2020) 102118.

[20] R. Mendelsohn, C.R. Flach, Infrared reflection-absorption spectroscopy of lipids, peptides, and proteins in aqueous monolayers, Curr. Top. Membr. 52 (2002) 57-88.

[21] K. Kim, S.Q. Choi, J.A. Zasadzinski, T.M. Squires, Nonlinear chiral rheology of phospholipid monolayers, Soft Matter 14 (2018) 2476-2483.

[22] D. Matyszewska, S. Moczulska, Effect of pH on the interactions of doxorubicin with charged lipid monolayers containing 1,2-dimyristoyl-sn-glycero-3-phospho-L-serine - An important component of cancer cell membranes, Electrochim. Acta 280 (2018) 229-237.

[23] J.R. Helliwell, Concerning the measurement of charge density X-ray diffraction data at synchrotron sources: challenges and opportunities, Crystallogr. Rev. 23 (2017) 160.

[24] M. Elderdfi, A.F. Sikorski, Langmuir-monolayer methodologies for characterizing protein-lipid interactions, Chem. Phys. Lipids 212 (2018) 61-72.

[25] W.M. Pazin, G.C.M. Ruiz, O.N.d.O. Jr, C.J.L. Constantino, Interaction of Artepillin C with model membranes: Effects of pH and ionic strength, BBA - Biomembranes 1861 (2019) 410-417.

[26] B. Gzyl-Malcher, J. Handzlik, E. Klekowska, Temperature dependence of the interaction of prazosin with lipid Langmuir monolayers, Colloids Surf. B Biointerfaces 112 (2013) 171-176.

[27] J.R. Lu, R.K. Thomas, J. Penfold, Surfactant layers at the air/water interface: structure and composition, Adv. Colloid Interface Sci. 84 (2000) 143-304.

[28] L. Braun, M. Uhlig, R. von Klitzing, R.A. Campbell, Polymers and surfactants at fluid interfaces studied with specular neutron reflectometry, Adv. Colloid Interface Sci. 247 (2017) 130-148.

[29] T. Narayanan, H. Wacklin, O. Konovalov, R. Lund, Recent applications of synchrotron radiation and neutrons in the study of soft matter, Crystallogr. Rev. 23 (2017) 160-226.

[30] R.A. Campbell, H.P. Wacklin, I. Sutton, R. Cubitt, G. Fragneto, FIGARO: The new horizontal neutron reflectometer at the ILL, Europ. Phys. J. Plus 126 (2011) 107.

[31] R.A. Campbell, Recent advances in resolving kinetic and dynamic processes at the air/water interface using specular neutron reflectometry, Curr. Opin. Colloid Interf. Sci. 37 (2018) 49-60.

[32] R.A. Campbell, A. Tummino, B.A. Noskov, I. Varga, Polyelectrolyte/surfactant films spread from neutral aggregates, Soft Matter 12 (2016) 5304-5312.

[33] A. Tummino, J. Toscano, F. Sebastiani, B.A. Noskov, I. Varga, R.A. Campbell, Effects of aggregate charge and subphase ionic strength on the properties of spread polyelectrolyte/surfactant films at the air/ water interface under static and dynamic conditions, Langmuir 34 (2018) 2312−2323.

[34] A. Angus-Smyth, R.A. Campbell, C.D. Bain, Dynamic adsorption of weakly interacting polymer/surfactant mixtures at the air/water interface, Langmuir 28 (2012) 12479−12492.

[35] K.R. Hossain, S.A. Holt, A.P.L. Brun, H.A. Khamici, S.M. Valenzuela, X‐ ray and neutron reflectivity study shows that CLIC1 undergoes cholesterol-dependent structural reorganization in lipid monolayers, Langmuir 33 (2017) 12497-12509.

[36] D. Matyszewska, E. Nazaruk, R.A. Campbell, Interactions of anticancer drugs doxorubicin and idarubicin with lipid monolayers: New insight into the composition, structure and morphology, J. Colloid Interface Sci. 581 (2021) 403–416.

[37] K.C. Thompson, A.R. Rennie, M.D. King, S.J.O. Hardman, C.O.M. Lucas, C. Pfrang, B.R. Hughes, A.V. Hughes, Reaction of a phospholipid monolayer with gas-phase ozone at the air-water interface: Measurement of surface excess and surface Ppessure in real time, Langmuir 26 (2010) 17295–17303.

[38] C. Pfrang, F. Sebastiani, C.O.M. Lucas, M.D. King, I.D. Hoare, D. Chang, R.A. Campbell, Ozonolysis of methyl oleate monolayers at the air–water interface: oxidation kinetics, reaction products and atmospheric implications, Phys. Chem. Chem. Phys. 16 (2014) 13220-13228.

[39] R.M.A. Azzam, N.M. Bashara, Ellipsometry and Polarized Light, North-Holland, New York, 1977.

[40] H. Motschmann, R. Teppner, Ellipsometry in Interface Science, Studies in Interface Science2001, pp. 1-42.

[41] J. Meunier, Light Scattering by Liquid Surfaces and Complementary Techniques, Marcel Dekker, New York, 1992.

[42] R.A. Campbell, J.C. Ang, F. Sebastiani, A. Tummino, J.W. White, Spread films of human serum albumin at the air-water interface: Optimization, morphology, and durability, Langmuir 31 (2015) 13535-13542.

[43] D. Ducharme, J.-J. Max, C. Salesse, R.M. Leblanc, Ellipsometric study of the physical states of phosphatidylcholines at the air-water interface, J. Phys. Chem. 94 (1990) 1925-1932.

[44] A. Poirier, A. Banc, A. Stocco, M. In, L. Ramos, Multistep building of a soft plant protein film at the air-water interface, J. Colloid Interface Sci. 526 (2018) 337–346.

[45] D. Beaglehole, Ellipsometric study of the surface of simple liquids, Physica 100B (1980) 163-174.

[46] F. Sebastiani, R.A. Campbell, C. Pfrang, Complementarity of neutron reflectometry and ellipsometry for the study of atmospheric reactions at the air–water interface, RSC Adv. 5 (2015) 107105–107111.

[47] T.L. Crowley, A uniform kinematic approximation for specular reflectivity, Physica A 195 (1993) 354-374.

[48] R.A. Campbell, Y. Saaka, Y. Shao, Y. Gerelli, R. Cubitt, E. Nazaruk, D. Matyszewska, M.J. Lawrence, Structure of surfactant and phospholipid monolayers at the air/water interface modeled from neutron reflectivity data, J. Colloid Interface Sci. 531 (2018) 98–108.

[49] J.H. Lakey, Recent advances in neutron reflectivity studies of biological membranes, Curr. Opin. Colloid Interface Sci. 42 (2019) 33–40.

[50] M.W.A. Skoda, Recent developments in the application of X-ray and neutron reflectivity to soft-matter systems, Curr. Opin. Colloid Interface Sci. 42 (2019) 41-54.

[51] O. Pabois, C.D. Lorenz, R.D. Harvey, I. Grillo, M.M.-L. Grundy, P.J. Wilde, Y. Gerelli, C.A. Dreiss, Molecular insights into the behaviour of bile salts at interfaces: a key to their role in lipid digestion J.Colloid Interface Sci. 556 (2019) 299-277.

[52] M.D. Phan, O.I. Korotych, N.G. Brady, M.M. Davis, S.K. Satija, J.F. Ankner, B.D. Bruce, X-ray and neutron reflectivity studies of styrene-maleic acid copolymer interactions with galactolipid-containing monolayers, Langmuir 36 (2020) 3970−3980.

[53] A. Nelson, Co-refinement of multiple-contrast neutron/X-ray reflectivity data using MOTOFIT, J. Appl. Crystallogr. 39(2) (2006) 273-276.

[54] A. Kabalnov, D. Klein, T. Pelura, E. Schutt, J. Weers, Dissolution of multicomponent microbubbles in the blood stream: 1. Theory, Ultrasound Med. Biol. 24 (1998) 739-749.

[55] M.P. Krafft, V.B. Fainerman, R. Miller, Modeling of the effect of fluorocarbon gases on the properties of phospholipid monolayers and the adsorption dynamics of their aqueous solutions or dispersions, Colloid Polym Sci. 293 (2015) 3091-3097.

[56] A.M.A. Dias, C.M.B. Gonçalves, A.I. Caço, L.M.N.B.F. Santos, M.M. Pineiro, L.F. Vega, J.A.P. Coutinho, I.M. Marrucho, Densities and vapor pressures of highly fluorinated compounds, J. Chem. Eng. Data 2005, 50, 50 (2005) 1328-1333.

[57] V.E. Stiles, G.H. Cady, Physical properties of perfluoro-n-hexane and perfluoro-2-methylpentane, J. Am. Chem. Soc. 74 (1952) 3771-3773.

[58] D.G. LeGrand, J. G. L. Gaines, The Polarizability of some deuterated hydrocarbons, J. Phys. Chem. 98 (1994) 4842-4844.

[59] F. Gerber, M.P. Krafft, T.F. Vandamme, M. Goldmann, P. Fontaine, Preventing crystallization of phospholipids in monolayers: a new approach to lung surfactant therapy, Angew. Chem. Int. Ed. 44 (2005) 2749-2752.

[60] F. Gerber, M.P. Krafft, T.F. Vandamme, M. Goldmann, P. Fontaine, Fluidization of a dipalmitoylphosphatidylcholine monolayer by fluorocarbon gases: potential use in lung surfactant therapy, Biophys. J. 90 (2006) 3184-3192.

[61] U.K. Basak, A. Datta, Dynamics driven by lipophilic force in Langmuir monolayers: In-plane and out-of-plane growth, Phys. Rev. E Stat. Nonlin. Soft Matter Phys. 91 (2015) 042405.

[62] N.O. Petersen, P.A. Kroon, M. Kainosho, S.I. Chan, Thermal phase transition in deuterated lecithin bilayers, Chem. Phys. Lipids 14 (1975) 343-349.

[63] F. Foglia, D.J. Barlow, F.C. Szoka, Z. Huang, S.E. Rogers, M.J. Lawrence, Structural studies of the monolayers and bilayers formed by a novel cholesterol-phospholipid chimera, Langmuir 27 (2011) 8275–8281.

[64] E. Madrid, S.L. Horswell, Effect of deuteration on phase behavior of supported phospholipid bilayers: A spectroelectrochemical study, Langmuir 31 (2015) 12544−12551.

[65] A. Luchini, R. Delhom, B. Demé, V. Laux, M. Moulin, M. Haertlein, H. Pichler, G.A. Strohmeier, H. Wacklin, G. Fragneto, The impact of deuteration on natural and synthetic lipids: A neutron diffraction study, Colloids Surf. B Biointerfaces 168 (2018) 126–133.

[66] M. Thoma, M. Schwendler, H. Baltes, C.A. Helm, T. Pfohl, H. Riegler, H. Möhwald, Ellipsometry and X-ray reflectivity studies on monolayers of phosphatidylethanolamine and phosphatidylcholine in contact with n-dodecane, n-hexadecane, and bicyclohexyl, Langmuir 12 (1996) 1722-1728.

[67] G. Bryant, M.B. Taylor, T.A. Darwish, A.M. Krause-Heuer, B. Kent, C.J. Garvey, Effect of deuteration on the phase behaviour and structure of lamellar phases of phosphatidylcholines –

Deuterated lipids as proxies for the physical properties of native bilayers, Colloids Surf. B Biointerfaces 177 (2019) 196–203.

[68] A. Briddick, P. Li, A. Hughes, F. Courchay, A. Martinez, R.L. Thompson, Surfactant and plasticizer segregation in thin poly(vinyl alcohol) films, Langmuir 32 (2016) 864−872.